# High-purity magnesium pin enhances bone consolidation in distraction osteogenesis via regulating Ptch protein activating Hedgehog-alternative Wnt signaling

Musha Hamushan [a], Weijie Cai [a], Yubo Zhang [a], Zun Ren [a], Jiafei Du [a], Shaoxiang Zhang [b], Changli Zhao [c], Pengfei Cheng [a], Xiaonong Zhang [b,c,***], Hao Shen [a,**], Pei Han [a,*]

[a] *Orthopaedic Department, Shanghai Jiao Tong University Affiliated Sixth People's Hospital, Shanghai, 200233, China*
[b] *Suzhou Origin Medical Technology Co. Ltd, Suzhou, 215513, China*
[c] *School of Materials Science and Engineering, Shanghai Jiao Tong University, Shanghai, 200240, China*

## ABSTRACT

Magnesium alloys are promising biomaterials for orthopedic implants because of their degradability, osteogenic effects, and biocompatibility. Magnesium has been proven to promote distraction osteogenesis. However, its mechanism of promoting distraction osteogenesis is not thoroughly studied. In this work, a high-purity magnesium pin developed and applied in rat femur distraction osteogenesis. Mechanical test, radiological and histological analysis suggested that high-purity magnesium pin can promote distraction osteogenesis and shorten the consolidation time. Further RNA sequencing investigation found that alternative Wnt signaling was activated. In further bioinformatics analysis, it was found that the Hedgehog pathway is the upstream signaling pathway of the alternative Wnt pathway. We found that Ptch protein is a potential target of magnesium and verified by molecular dynamics that magnesium ions can bind to Ptch protein. In conclusion, HP Mg implants have the potential to enhance bone consolidation in the DO application, and this process might be via regulating Ptch protein activating Hedgehog-alternative Wnt signaling.

## 1. Introduction

Bone defects are common complications caused by trauma, infections, tumors, deformities, etc., and the clinical treatment is very challenging [1]. The distraction osteogenesis (DO) technique has been used in orthopedics since the 1960s and achieved good clinical results [2]. The DO procedure comprises three phases: the latency phase after surgery, the distraction phase where in the stable and slow distraction can create a mechanobiological environment for stimulating new bone regeneration, and the consolidation phase for the achievement of sufficient quality of new bones [3].The DO growth pattern is similar to fetal tissue [4,]. The DO technology is more and more widely used at present, but a common problem is the slow calcification of new bone formation [6]. That causes patients increased complications such as infection and joint stiffness etc. [7] These all lead to prolonged treatment cycles, which bring great inconvenience to patients' life and work, increase the economic and mental burden, and limit the clinical application of DO

[8]. Therefore, improving the speed and quality of new bone formation and calcification in the process of DO and shortening the fixation time are urgent problems to be solved clinically [9].

The degradable magnesium (Mg) metal has been a research hotspot in recent years [10]. Mg alloys are expected to become osteoconductive and biodegradable orthopedic implants and applied in clinical conditions [11,12]. In our previous study, we found that high-purity magnesium bone screws and interface screws have good osteogenic calcification effects under fracture stress and in bone tunnels, and found that this phenomenon is achieved by magnesium ion activating BMP-2 and VEGF [13,14]. In a recent study, we conducted a series of studies on the effect and mechanism of magnesium on distraction osteogenesis. The high-purity magnesium (HP Mg) pin was used as the intramedullary guide for the rat femoral distraction osteogenesis model, and the stainless steel (SS) group and the blank group were used as controls. We found that HP Mg intramedullary pin could enhance bone formation and consolidation in a rat DO model. This process might be via the regulation
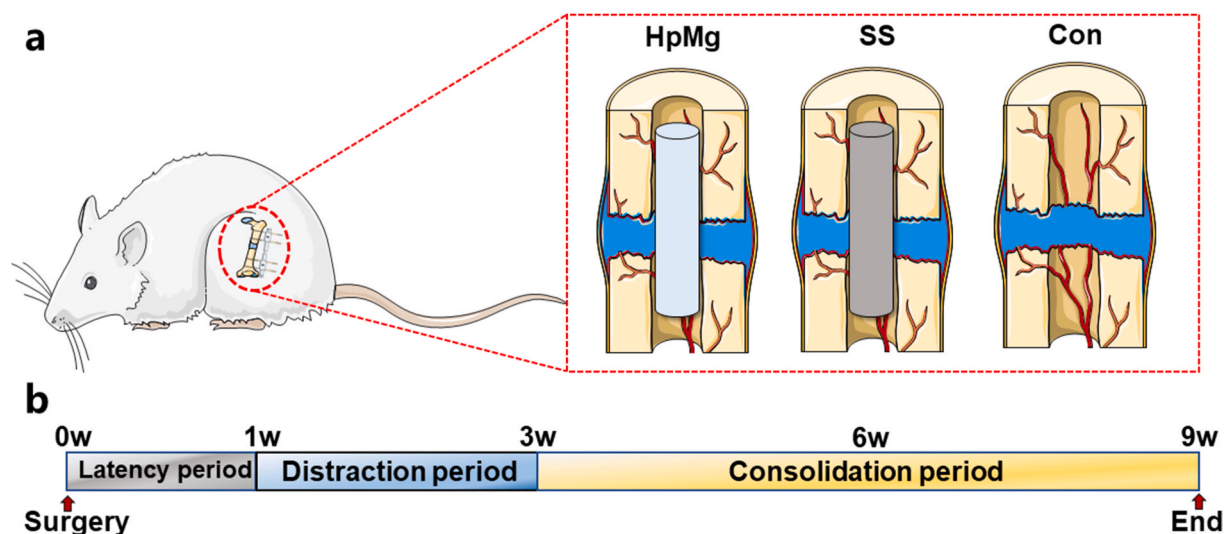
**Fig. 1.** a: The grouping of rat femur DO model. b: Timeline for distraction protocol.

of Von Hippel–Lindau/hypoxia inducible factor-1a/vascular endothelial growth factor signaling (VHL/HIF-1α/VEGF signaling) [15].

Although in the previous research we report that HP Mg pin enhances bone consolidation in distraction osteogenesis model through activation of the VHL/HIF-1α/VEGF signaling, its mechanism investigation is limited to angiogenesis. Whether HP Mg can promote distraction osteogenesis through other pathways is still unknown. To this end, we took new bone tissue for high-throughput transcriptome sequencing (RNA-seq) in the middle of the consolidation phase and explore the mechanism through bioinformatics analysis, molecular dynamics and other methods.

## 2. Materials and methods

### 2.1. Materials preparation

The HP Mg pins were supplied by Suzhou Origin Medical Technology Co.Ltd., China. The pins were designed with a total length of 5 mm, diameter of 1 mm. All samples were rinsed in acetone and ethanol successively, washed in distilled water, and then sterilized with 29 kGy of 60 Co radiation.

### 2.2. Animals

Sprague- Dawley rats (12-week old male, purchased from the Experimental Animal Center of Shanghai Jiao Tong University Affiliated Sixth People's Hospital) were chosen as the research subjects. Animals were housed in a light/dark and temperature-controlled room. The distraction osteogenesis model in rats was approved by the Ethics Committee of the Sixth People's Hospital Affiliated with the School of Medicine of Shanghai Jiao Tong University (Animal Committee Approval No. 2019-0187). All procedures that involved animals followed the Care and Use Committee guidelines of the Sixth People's Hospital Affiliated with the School of Medicine of Shanghai Jiao Tong University. All rats were randomly separated into three groups: HP Mg pin group, SS (1 mm Kirschner wire) group (positive control) and control group (negative control) (Fig. 1a). Each group was further divided into three subgroups according to implantation time of 3,6 and 9 weeks.

### 2.3. Surgery and distraction protocol

All surgical operation was performed by the same skilled orthopedic surgeon. Total 54 rats were used. The rat femoral distraction osteogenesis models were been made as previously described. Briefly, the rats

were anesthetized with 4% pentobarbital sodium. The lateral aspect of the right hind limb was shaved and sterile-draped. The skin over the lateral aspect of the hip joint to the lateral side of the knee joint was incised, the fascia cut longitudinally, and the femur exposed. The periosteum was incised longitudinally and retracted carefully. Four self-tapping screws (stainless steel) were inserted into the femur at a right angle to the long axis of the bone, and custom unilateral external fixator was applied. A transverse osteotomy was performed in the middle of the diaphysis between the second and the third screw. HP Mg or SS pin was inserted into the bone marrow cavity for HP Mg group and SS group. The bone ends were reduced, and the muscle, fascia, and skin sutured [15]. Distraction osteogenesis was divided into 3 phases: the latency period of 7 days after surgery; the active distraction period of 2 weeks, during which gradual distraction was initiated at a rate of 0.25 mm/12 h (total 7 mm); and the consolidation period of 6 weeks, during which the external distractor was held in situ as a fixator. (Fig. 1b). The rats in three groups were sacrificed on the 3rd, 6th and 9th week post-operation and samples were collected.

### 2.4. Plane radiographic evaluation and micro-computed tomography (micro-CT) evaluation

Digital X-ray machine (Digital Diagnost, Philips, Amsterdam, Netherlands) was used for X-ray examination of the distraction zone until sacrifice under general anesthesia for 3,5,7,9 weeks after surgery in 9 weeks group for continuous observation.

Micro-CT (μCT 80; SCANCO Medical AG, Bassersdorf, Switzerland) imaging was performed to analyze the new bone formation, bone consolidation and in vivo degradation of the HP Mg intramedullary pin. n = 6 for each after the animals had been euthanized. the femurs were harvested and evaluated by micro-CT. The region of interest (ROI) was defined as the part of diaphysis between the 2nd and 3rd screw. Three-dimensional (3D) reconstruction was performed, and bone mineral density (BMD), BV (bone volume)/TV (total volume), trabecular thickness (Tb. Th) and bone volume surrounding pin were quantitatively analyzed using all 600 slides of 2D images.

### 2.5. Biomechanical testing

At 9 week 5 specimens from each group were randomly selected for torsional biomechanical testing. After the rats were killed by excessive anesthesia, the traction and extension of the femur and the left femur of the normal rat were immediately taken out, and the fixed steel needle and surrounding soft tissue and periosteum were carefully removed, the

femoral head was removed, and both ends of the femur were embedded in polymethacrylic acid. Salt resin material state. After the embedding is stable, the specimen is mounted on the three-point bending device (Instron5566; Instron, Norwood, MA, USA). The femur samples were loaded in the anterior-posterior direction at a loading rate of 1 mm/min until failure. Ultimate loading and energy to failure were analyzed and normalized to the contralateral femur.

### 2.6. Histological analysis

After the micro-CT images had been obtained, the femurs were decalcified in moderate demineralized solution (15%EDTA solution). After complete decalcification, sample dehydration, transparency and paraffin embedding were successively performed. All samples were consecutively cut into 5 μm thick slices and then were stained with hematoxylin & eosin (H&E) and Saffron solid green stains for morphology observation.

### 2.7. RNA-seq and bio-informatic analysis

At 6 week 4 specimens from each group were randomly selected for RNA-seq analysis. Total RNA from each sample was extracted using an RNeasy Mini Kit (Qiagen, Hilden, Germany), and library preparation was conducted using an MGI Easy™ mRNA Library Prep Kit (BGI, Inc., Wuhan, China) following manufacturer's instructions and the previous work and [16]. The sequencing library was used for cluster generation and sequencing on the BGISEQ-500 system (BGI). The sequencing was repeated 10 times, and the differentially expressed genes (DEGs) were defined as foldchange$\geq$2 and p value $\leq$ 0.05. The reference genes were from Rattus norvegicus-UCSC_rn6 (ftp://hgdown-load.cse.ucsc.edu/goldenPath/rn6) Kyoto Encyclopedia of Genes and Genomes (KEGG) pathway enrichment analysis was performed using DAVID (https://david.ncifcrf.gov). The regulatory network and related transcription factors of related genes analysis was performed using the GCBI gene radar (https://www.gcbi.com.cn). These results are further compared with previous DEGs.

### 2.8. RT-PCR

The effects of Hp Mg on the expression of Hedgehog-alternative Wnt signaling were detected using RT-PCR. Total RNA was extracted using Trizol reagent (Invitrogen, Carlsbad, CA). cDNA was synthesized using Revert Aid First Strand cDNA Synthesis Kit (Invitrogen, USA). Quantitative PCR was performed mRNA expression levels were analyzed using the $2-\Delta\Delta Ct$ method with GAPDH as the housekeeping gene. The primers (BioTNT, Shanghai, China) used in this study were listed in Table 1.

### 2.9. Western blot

Distraction callus protein was extracted with the Protein Extraction Kit (KeyGen, Nanjing, China). Protein concentration was analyzed with the BCA Protein Assay Reagent Kit. Each sample protein was analyzed by electrophoresis in 10% acrylamide gels (with SDS) and transferred to transfer buffer at RT with shaking. To block the non-specific binding site (without SDS), the membrane was immersed into 5% non-fat milk in Tris-buffered saline solution for 2 h. The membrane was incubated for 2 h with primary antibodies against Wnt5b (Abcam), YAP (yes-associated protein) (Abcam), Wnt3a (Abcam), β-catenin (Abcam), Runx2 (Runt-related transcription factor 2) (Abcam), Ptch1(Patched1) (Abcam) and Gli1 (glioma associated oncogene homolog 1) (Abcam) antibodies in 10 mL of 5% non-fat milk in TBST solution. Each membrane was probed with β-actin (Abcam) as a loading control.

### 2.10. Immunohistochemical analysis

Following experiments, the expression of in the distraction region was analyzed by immunohistochemical staining. Immunohistochemistry staining was performed using primary antibodies to rabbit Wnt5b, YAP Wnt3a, β-catenin, Runx2, Ptch1 and Gli1 overnight at 4 °C. Then, a horseradish peroxidase-streptavidin detection system (Dako, USA) was used, followed by counterstaining with hematoxylin. The number of positively stained cells in the whole distraction regenerated in three sequential sections (50, 150, and 250 lm) per specimen per rat were counted and compared statistically.

### 2.11. Molecular dynamics simulation

The molecular dynamics simulation was performed using GROMACS 5.1.43 software, the initial structure was using Ptch1- Sonic Hedgehog complex (PDB ID 6OEV), the missing fragments in Ptch1 were completed using Modeller 9.18 4, and the energy was minimized to eliminate the spatial position Hinder. The pKa value of the residue is predicted using PROPKA 3.15 software, and the protonation state is assigned according to the pKa value under the condition of pH = 7.4, and carefully checked. For protein, use Amber ff14SB6 force field, add 0.15 mol/L Na + or Mg2+ ion to the system, Mg2+ use Amber ff14SB default force field parameter, add chloride ion to neutralize the charge in the final system, about 70 000 TIP3P water molecules are used for cube The solvation of the proteins in the cycle box has an average density of 1 kg/m3. All non-bonding interactions are clearly calculated to a distance of 10 Å. The PME method is used to handle remote static electricity. The entire system performs 50 000 steps of energy minimization on the steepest descent method. Once the minimization is completed, the system is heated to 300 K under the NVT ensemble, using a force of 1000 J/mol to bind the protein heavy atoms, and running for 250 ps. Under the NPT ensemble, the simulation was performed at a pressure of 300 K and 1

**Table 1**
Primers used in this study for RT-PCR.

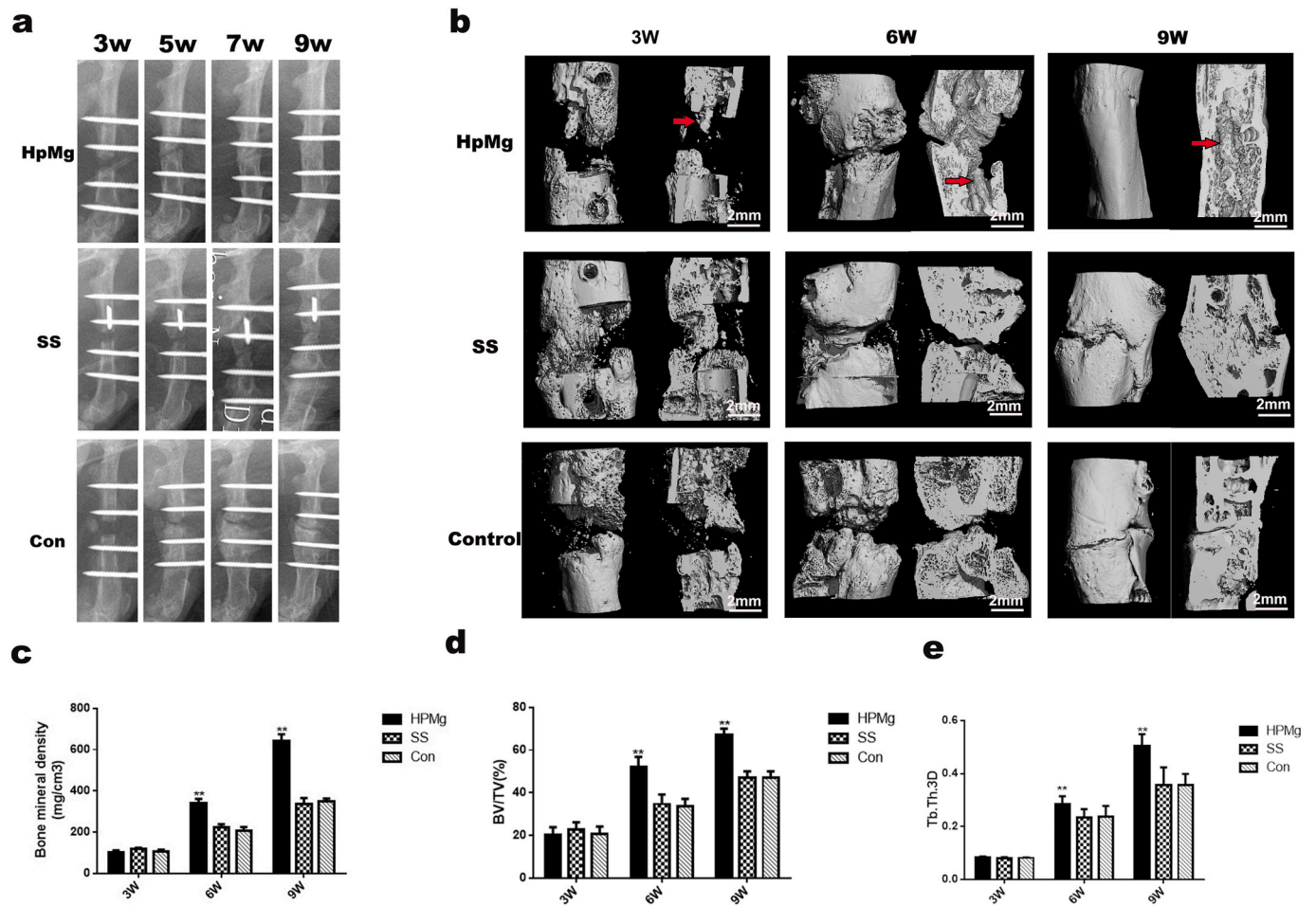| Genes | Forward primer (5′–3′) | Reverse primer (5′–3′) |
|---|---|---|
| Yap | 5′ CTG ATG ATG TAC CAT TGC CAG 3′ | 5′ CTG CCA TGT TGT TGT CTG ATC 3′ |
| Wnt5b | 5′ TCA TCT GAG TAC ACA TGG CAG 3′ | 5′ ATC TCT TAC GGT CAC CAG TCA 3′ |
| FZD | 5′ CGA CGG CTC CAT GTT CTT C 3′ | 5′ GCA CCG ACC ATG TGA GGA T 3′ |
| Wnt3a | 5′ ATG AAC TTC GTG GAC ATG GAG 3′ | 5′ GCT CTG GGA ATG GAA TAG GTC3′ |
| β-catenin | 5′ GCC ACA GGA CTA CAA GAA ACG 3′ | 5′ ATC AGC AGT CTC ATT CCA AGC 3′ |
| Runx2 | 5′ ATC ATT CAG TGA CAC CAC CAG 3′ | 5′ GTA GGG GCT AAA GGC AAA AG 3′ |
| shh | 5′ GACCCAACTCCGATGTGTTCC 3′ | 5′ATATAACCTTGCCTGCTGTTGCTG 3′ |
| ihh | 5′ TCAGCGATGTGCTCATTTTC 3′ | 5′ CCTCGTGAGAGGAGCTAGG 3′ |
| Smo | 5′ TCC AGC GAG ACC CTA TCC T 3′ | 5′ AAC CAC ACT ACT CCA GCC ATC 3′ |
| Ptch1 | 5′ TTG GTT GTG GGT CTC CTC A 3′ | 5′ CTC CTA TCT TCT GGC GGG TAT 3′ |
| Gli1 | 5′ AAC CCC TCC TCT CAT TCC ACA 3′ | 5′ TTC TGC CCT CCC ACA ACA A 3′ |
| Gli2 | 5′ ATC CCT AAC TCC TCA GCC ATC 3′ | 5′ CAG CCT CCG TTC TGT TCA T 3′ |
| Gapdh | 5′ AAA CCC ATC ACC ATC TTC CAG 3′ | 5′ CTC CAC GAC ATA CTC AGC ACC 3′ |

**Fig. 2.** HP Mg accelerated bone consolidation during distraction osteogenesis in rats. a:X-ray images of the distraction regenerate at 3,5,7 and 9 weeks after distraction. b: Representative 3D micro-CT images of the distraction zone after surgery 3,6 and 9 weeks (Red arrows: HP Mg pins). c, d, e: Quantitative analysis of micro-CT data showed higher values of BMD, BV/TV and Tb.Th in the Hp Mg group at consolidation phase (**p < 0.01). (For interpretation of the references to color in this figure legend, the reader is referred to the Web version of this article.)
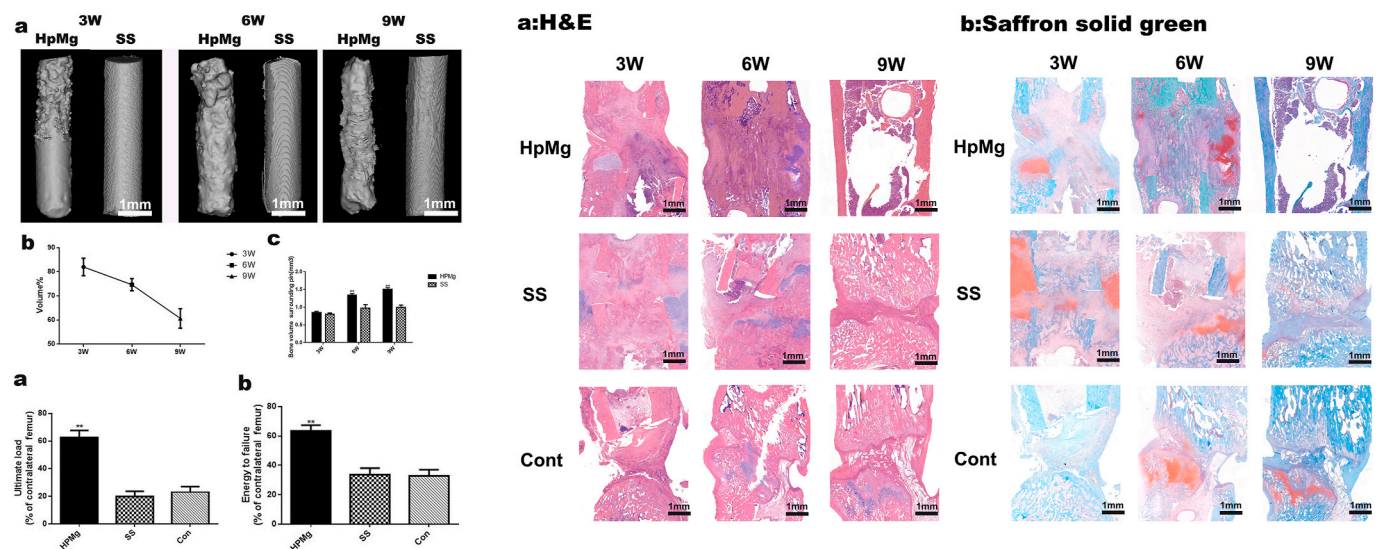


**Fig. 3.** a: In vivo 3D micro-CT images of the HP Mg and SS pins. b: Volume change of intramedullary HP Mg pins. c: Bone volume surrounding HP Mg and SS pins (**p < 0.01). d, e: Mechanical tests (ultimate load and energy to failure) of the distracted femur. The values were normalized to the corresponding contralateral normal femur (**p < 0.01). f:H&E staining HP Mg group enhanced bone consolidation in comparison with the SS and control group. g: In Saffron solid green, at 6 and 9weeks chondrocytes cartilage were evident in the SS and control groups compared to the HP Mg group. (For interpretation of the references to color in this figure legend, the reader is referred to the Web version of this article.)

**Fig. 4.** a: Summary of DEGs. Red color represents up-regulated DEGs. Blue color represents down-regulated DEGs. b, c, d: Volcano plot. Red points represent up-regulated DEGs. Blue points represent down-regulated DEGs. Gray points represent non-DEGs. e: Venn diagram of DEGs. f: Bubble chart showing top 20 enriched pathways in the KEGG. (For interpretation of the references to color in this figure legend, the reader is referred to the Web version of this article.)
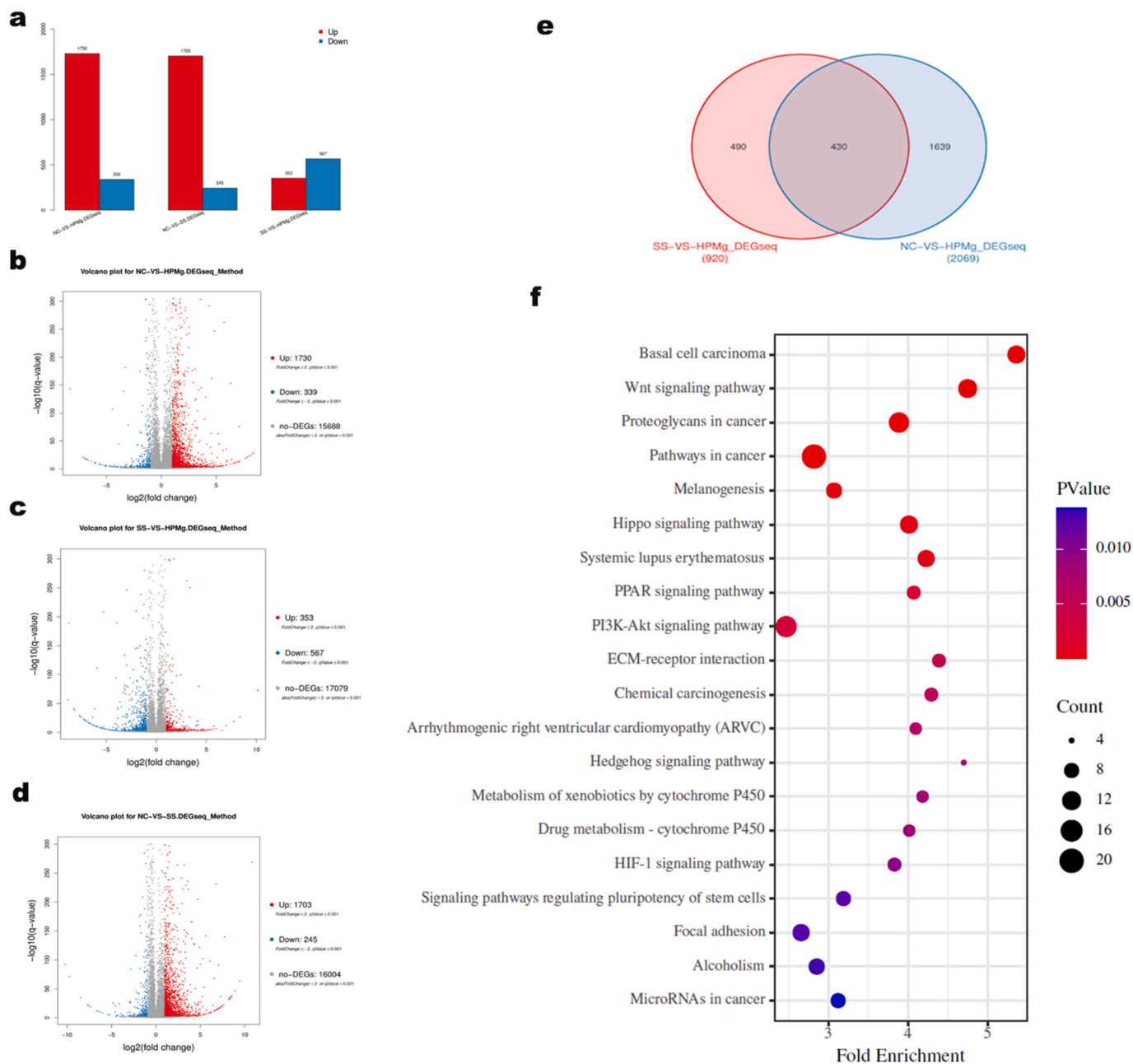
atm, running 15 ns for density balancing, and also using a force of 1000 J/mol to constrain protein-heavy atoms. Finally, a molecular dynamics simulation of 70 ns was performed at 300 K with a time step of 2 fs. The constraints of all bonds and water molecules were performed using LINCS and SETTLE algorithms, respectively. The computing hardware is accelerated by I7 8700 K and 1080ti GPU, using skeleton atomic co-ordinates for root mean square deviation (RMSD), root mean square fluctuation (RMSF) and radius of gyration (Rg) calculations, and using VMD 1.9.37 and PyMol 1.7.2.1 for visualization Check and generate a movie, use the DSSP program to analyze changes in secondary structure.

### 2.12. Statistical analysis

The data are expressed as the mean ± standard deviation (SD) from at least three independent experiments. The results were analyzed via Student's t-test or one-way analysis of variance (ANOVA), followed by the least significant difference (LSD) test for multiple comparisons using SPSS 19.0 software (SPSS Inc., Chicago, IL, USA). $p < 0.05$ indicated significant difference between groups.

## 3. Results

### 3.1. HP Mg pin accelerated new bone consolidation during DO in rats

In general observation rats completely recovered from surgical procedures and survived to the completion of the experiment without detectable adverse effects from HP Mg pin. There were no significant body weight changes in groups.

In the radiographic and micro-CT analysis, new bone consolidation progression was monitored by X-ray radiography and micro-CT. Serial
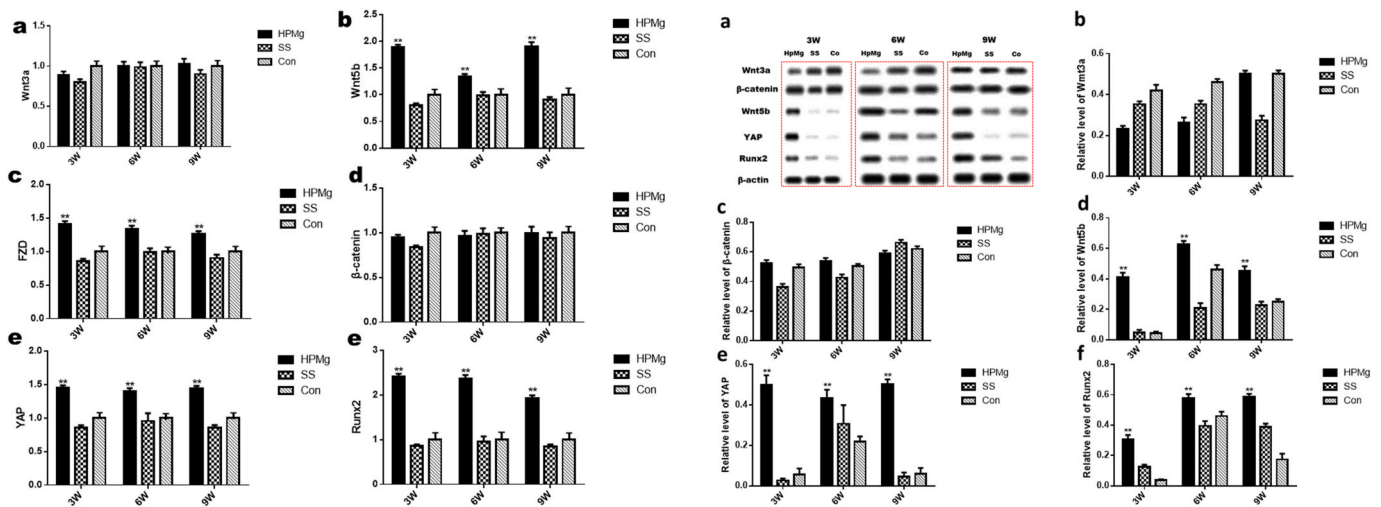
**Fig. 5.** a–f: RT-PCR analysis of mRNA in Wnt signaling. HP Mg induced Wnt5b, YAP, FZD and Runx2 levels in alternative Wnt signaling and have no difference in Wnt3a and β-catenin expression level in canonical Wnt signaling (**p < 0.01). g: Western blot analysis showed that HP Mg induced Wnt5b, YAP and Runx2 levels in alternative Wnt signaling and have no difference in Wnt3a and β-catenin expression level in canonical Wnt signaling. h–i: Relative expression level (**p < 0.01).

radiographic images across the time-course of DO demonstrated the progression of bone consolidation. At 3 weeks after surgery (the beginning of consolidation), callus formation was negligible. During consolidation period, more callus formations were evident in the HP Mg group comparing to the SS and control groups; at 9 weeks after surgery, bone formation increased in all group, but the quality of the newly formed bone in terms of volume and continuity of the callus, was better in the HP Mg group comparing to the other two groups (Fig. 2a). Similar observations were confirmed by the micro-CT examination (Fig. 2b). The 3D reconstructions revealed no differences in callus formation between 3 groups at week 3. However, the HP Mg group had higher newly mineralized bone quality than the control groups at Weeks 6; moreover, at week 9, the continuity of the marrow cavity in HP Mg group was almost completely remodeled, whereas the remodeling was ongoing in two control group. The BV/TV, BMD, Tb.Th and bone volume surrounding pin values were significantly higher in the HP Mg group than in the SS and control groups at 6 and 9 weeks (P < 0.01) (Fig. 2c,d,e) (Fig. 3c), suggesting the beneficial effects of HP Mg in promoting bone consolidation. The calculated volume loss of the HP Mg pin was stable, and pin volume decreased from $82.36 \pm 1.48$ mm$^3$ at 3 weeks to $73.39 \pm 1.39$ mm$^3$, $61.06 \pm 1.37$ mm$^3$, at, 6 and 9 weeks, respectively (Fig. 3a and b).

In mechanical testing, as shown in Fig. 3d and e, the mechanical testing showed a significant improvement in the ultimate load (p < 0.01), and energy to failure (p < 0.01), compared to those of the SS and control groups after they were normalized with respect to the contralateral femur at the end of the protocol.

In histological assessment, H&E staining of the distraction regenerates treated with HP Mg exhibited enhanced bone consolidation at 6 and 9 weeks after distraction in comparison with the SS and control group. In the images of Saffron solid green, at 6 and 9 weeks an increased areas of cartilage were evident in the SS and control groups compared to the HP Mg group, indicating that the newly formed chondrocytes have not been mineralized completely in these two groups (Fig. 3f and g).

### 3.2. HP Mg pin stimulated osteogenesis during DO in rats via alternative Wnt signaling

To explore the mechanism dictating the effect of HP Mg on DO, we conducted a statistical comparison of DEGs produced by tissues in three groups. We identified 1730 upregulated genes and 339 downregulated genes with the HP Mg group compared to the control group (Fig. 4a–d). We

353 upregulated genes and 567 downregulated genes with the HP Mg group compared to the SS group (Fig. 4a, c). 1703 upregulated genes and 245 downregulated genes with SS group compared to the control group (Fig. 4a, d). By taking intersection, we identified 430 genes, only differentially expressed in the HP Mg group (Fig. 4e).The differences between gene expression with different extract medium were evaluated by KEGG analysis. The top 20 KEGG pathways were selected based on the most significant fold enrichment (Fig. 4f). From this, we identified that the DEGs were significantly enriched in pathways associated with Wnt signaling (most obvious enrichment in osteogenesis-related pathways).

In order to verify the RNA-seq results, PCR detection results of Wnt pathway related genes were performed. The results showed that there were no significant differences in the expression of Wnt3a and β-catenin in the canonical Wnt pathway, while the Wnt5b (determined by DEGs), FZD, YAP and Runx2 in the alternative Wnt pathway all have high expression in HP Mg group (p < 0.01) (Fig. 5a–f).

To confirm the protein expression changes of the related genes, Western blot was performed on the same time course. The protein expression of Wnt5b, YAP and Runx2 increased at three time points. The protein expression of Wnt3a and β-catenin have no differences (p < 0.01) (Fig. 5g-l). Western blot results were consistent with the PCR analysis.

In further immunochemical analysis, the qualitative immunostaining results with Wnt5b, YAP and Runx2 antibodies revealed significant increase and Wnt3a and β-catenin antibodies revealed no difference in the HP Mg group compared to the other groups (p < 0.01) (Fig. 6).

### 3.3. HP Mg pin stimulated osteogenesis during DO in rats via hedgehog-alternative Wnt signaling

For Wnt5b, we further explored the upstream genes through gene radar and found that there is total of 25 genes. Further compared with the previous RNA-Seq DEGs, we found that only Gli1 and Gli2 in the hedgehog pathway were differentially expressed (Fig. 7d and e). It shows that the Hedgehog pathway is the upstream pathway of the alternative Wnt pathway activated by wnt5b.

In order to verify the RNA-seq results, PCR detection results of Hedgehog pathway related genes were performed. The results showed that there was no significant difference in the expression of the shh (Sonic hedgehog) and ihh (Indian hedgehog), while the Ptch1, Smo (smoothened), Gli1 and Gli2 all have high expression in the Hp Mg group (Fig. 7f–k).

**Fig. 6.** Immunohistochemistry images of distracted rat femur in three groups for Wnt5b, YAP, Runx2, Wnt3a and β-catenin at three, six, and nine weeks (a, b, e, f, i). The semiquantitative measurements showed that percentage of Wnt5b, YAP and Runx2 positive cells highly expressed in HP Mg group and Wnt3a and β-catenin positive cells have no differences in three groups (c, d, g, h, j) (**p < 0.01).

To confirm the protein expression changes of the related genes, Western blot was performed on the same time course (Fig. 7a–c). The protein expression of Ptch1 and Gli1 increased at three time points (p < 0.01). Western blot results were consistent with the PCR analysis.

In the further immunochemical analysis, the qualitative immuno-staining results with Ptch1 and Gli1 antibodies revealed a significant increase in the HP Mg group compared to the other groups (p < 0.01) (Fig. 8).

### 3.4. Magnesium ion stimulated hedgehog-alternative Wnt signaling via Ptch1 protein

Molecular dynamics simulation results show that Mg ion can bind to the Ptch1. It is particularly obvious that magnesium ion forms a coordination bond with acidic amino acid residues Glu592, Asp803 and Asp804 on the surface of Ptch1 protein, which stabilizes the structure of the 562–595 and 794–803 regions. In addition, it forms coordination bonds with other acidic residues Glu191, Glu188, Glu205, Asp782,

**Fig. 7.** a: Western blot analysis showed that HP Mg induced Ptch1 and Gli1 levels b–c: Relative expression level (**p < 0.01). d: Wnt5b gene radar analysis. e: RNA-seq results enrichment map of Hedgehog pathway. F-k: RT-PCR analysis of mRNA in Hedgehog signaling. HP Mg induced Ptch1, Smo, Gli1 and Gli2 levels and have no difference in shh and ihh expression levels (**p < 0.01).

Asp361, Asp105 and Asp787, which also plays an important role in stabilizing the structure of Ptch1 protein (Fig. 9a).

### 4. Discussion

In the present study, we applied the HP Mg pin in a rat femur DO model and demonstrated its potential to reduce the period of consolidation phase and permit the earlier removal of the external fixator. In the further mechanism study by RNA-seq detection, we found that alternative Wnt signaling was activated. When the ligand protein Wnt5b of alternative Wnt signaling was traced, it was found that its secretion is related to the Hedgehog signaling. In the study of magnesium target protein, Ptch1 protein was found to be its potent target protein.

In our results, three groups produced a similar quantity of new bones at the end of the distraction period. However, during the consolidation phase, the HP Mg group showed a faster consolidation speed. The BV/TV, BMD, Tb.Th and bone volume surrounding pin values detected by micro-CT analysis showed that the quality and quantity of bone tissue in

the regeneration space after HP Mg treatment were significantly improved (Fig. 2.) (Fig. 3c). Histological observations also show that the consolidation process has been almost completed in the HP Mg group at 9 weeks after surgery, which is significantly better than the two control groups (Fig. 3f, g). In addition, at the end of the experiment, the mechanical evaluation showed that the HP Mg group had a higher ultimate load and energy to failure compared to the two control groups (Fig. 3d and e). The HP Mg degradation rate results show that the HP Mg pins could provide continuous guiding within the process of DO and demonstrated steady degradation properties due to high purities. Together, these results indicate that HP Mg can significantly accelerate the consolidation during DO in rats.

In order to explore the mechanism, we took new bone tissue from 6 weeks group for RNA-seq analysis. By intersecting HP Mg relative control and SS groups differentially expressed genes, it was found that 430 genes were only differentially expressed in the HP Mg group. Enrichment analysis of the KEGG pathway was performed on differentially expressed genes (Fig. 4). KEGG pathway enrichment results showed that

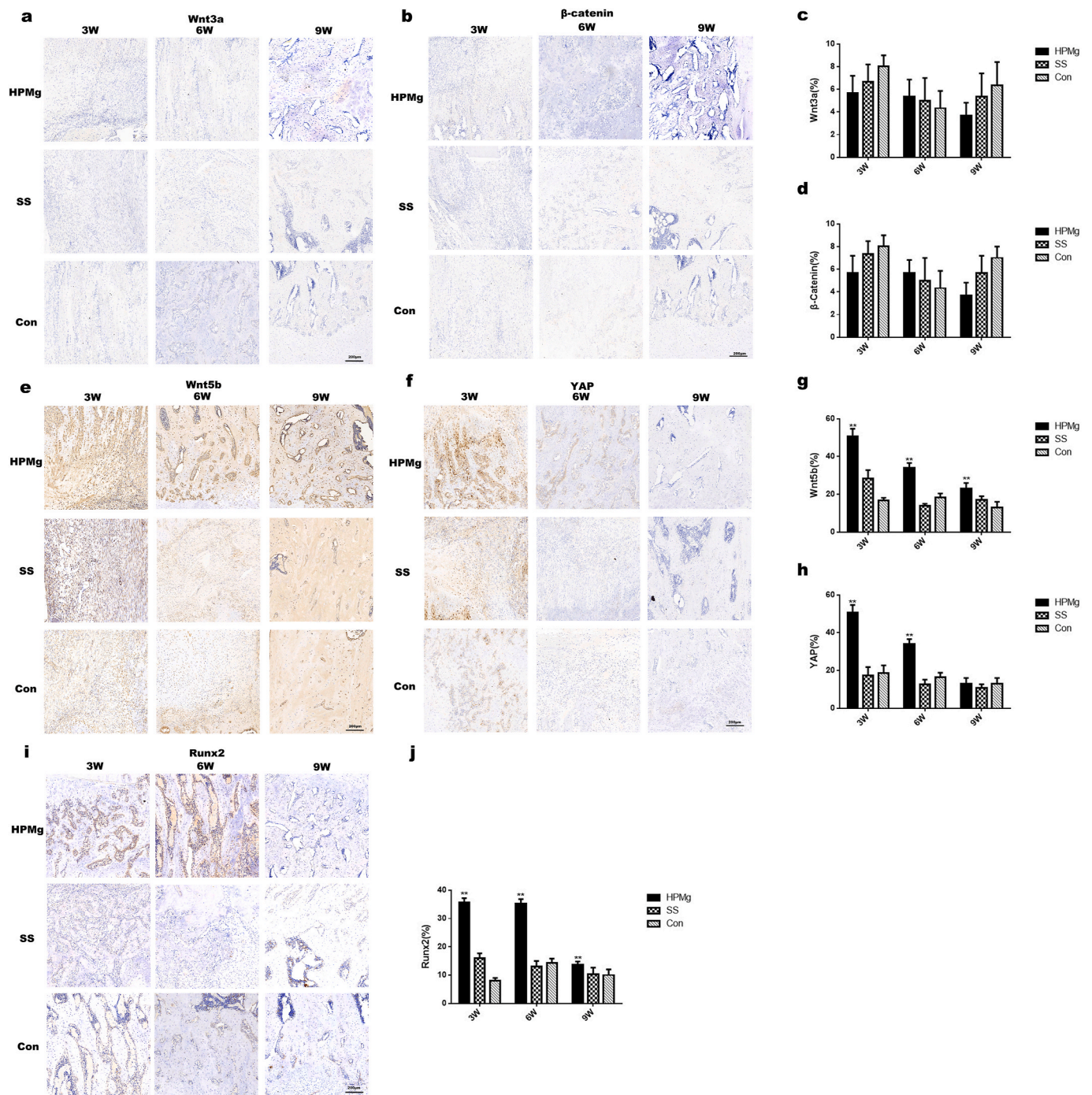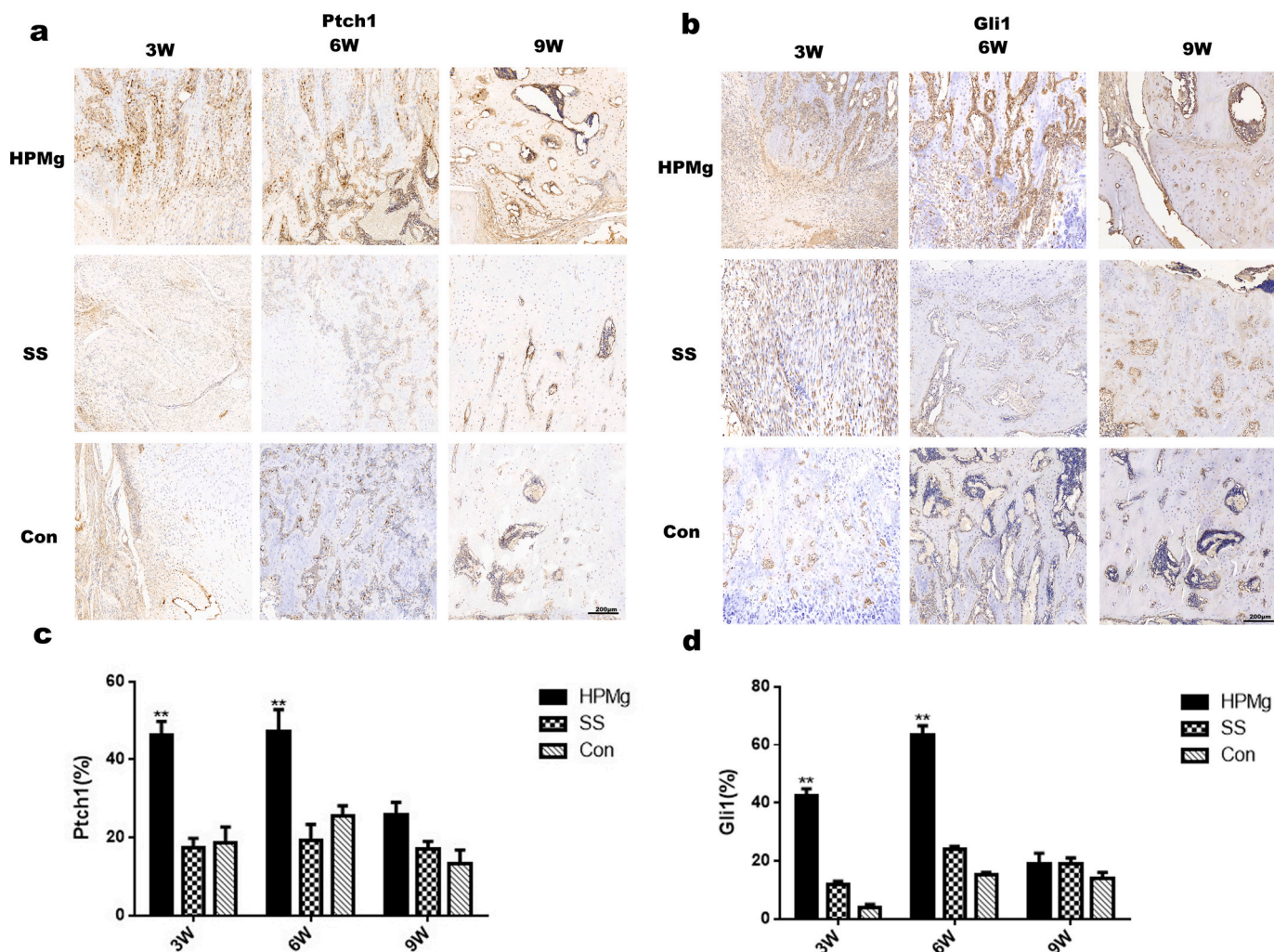**Fig. 8.** Immunohistochemistry images of distracted rat femur in three groups for Ptch1 and Gli1 at three, six, and nine weeks (a, b). The semiquantitative measurements showed that percentage of Ptch1 and Gli1 positive cells highly expressed in HP Mg group a (c, d) (**p < 0.01).

12 genes out of a total of 212 genes in the Wnt pathway were highly expressed in the HP Mg group, and the second obvious enrichment in all pathways. The Wnt pathway is one of the three major intracellular signal transduction cascades, which are all stimulated by certain extra cellular Wnt ligands, a group of 19 secreted glycoproteins [17]. The Wnt signaling is known to regulate bone formation through multiple mechanisms. Normally, activation of Wnt signaling will result in increase of bone formation and decrease of bone resorption [18,19]. In recent study, Chu-Chih Hung et al. suggest that Mg ion induces an osteogenic effect in the bone marrow space by activating the canonical Wnt signaling pathway, which in turn causes BMSCs to differentiate toward the osteoblast lineage [20]. However, in further research on canonical Wnt signaling's key genes, we found that the Wnt3a in the canonical Wnt signaling and its downstream β-catenin were not differentially expressed. The alternative Wnt signaling pathway is activated. Research by Park HW et al. showed that the alternative Wnt signaling stimulates membrane protein FZD through Wnt5b protein, further activates YAP/TAZ and incorporates into the nucleus to promote high expression of TEAD in the nucleus, thereby promoting the expression of Runx2 and other osteogenic genes and promoting osteogenesis [21]. We performed RT-PCR, Western blot and immunohistochemical analysis results verification on key genes in the Wnt signaling. The PCR results showed no differential expressions of Wnt3a and β-catenin in the canonical Wnt

pathway, while Wnt5b, YAP and Runx2 in the alternative Wnt signaling were all highly expressed in the HP Mg group. In consistency with these studies, our result showed that HP Mg promotes the expression level of Wnt5b, YAP, and Runx2 in the consolidation period according to the Western blot assay and immunochemical analysis increased in the HP Mg group (Figs. 5 and 6). Therefore, we proposed that magnesium promotes distraction osteogenesis consolidation through the alternative Wnt signaling instead of the canonical Wnt pathway.

Wnt5b, as an upstream ligand of alternative Wnt pathway, plays an important role in bone growth and fracture healing, especially in intrachondral osteogenesis. Studies by Ling IT et al. have shown that Wnt5b is involved in zebrafish cartilage formation and intra-cartilage osteogenesis [22]. In our result, Wnt5b was highly expressed in the HP Mg group. We further explored upstream genes through gene radar and compared with the previous RNA-Seq enrichment results, and found that the upstream genes of Gli1 and Gli2 were highly expressed. Both Gli1 and Gli2 are key nuclear transcription factors in the Hedgehog pathway. Hedgehog signaling pathway is a conservative and important signaling pathway that participates in various biological metabolism processes in the body [23]. Studies have shown that the Hedgehog signaling pathway is involved in metabolic processes such as bone formation, metabolism and fracture healing [23,24]. Inhibition of the Hedgehog pathway can lead to fracture nonunion or delayed healing [25,26]. The hedgehog
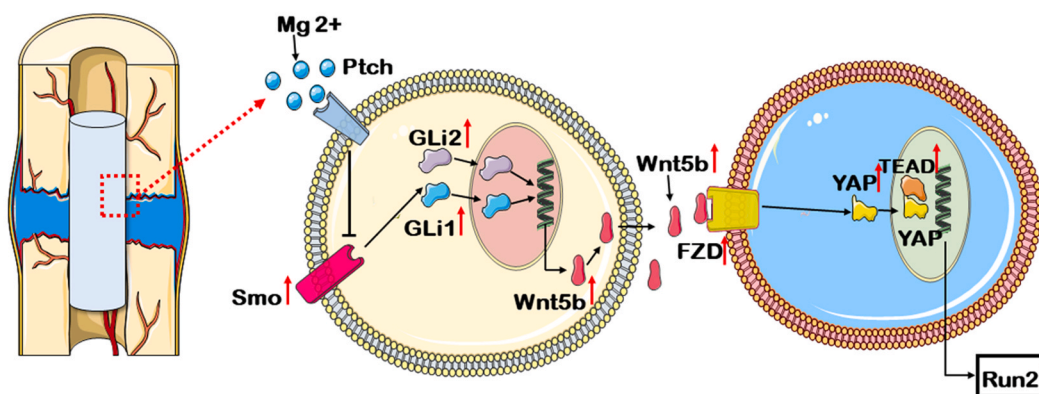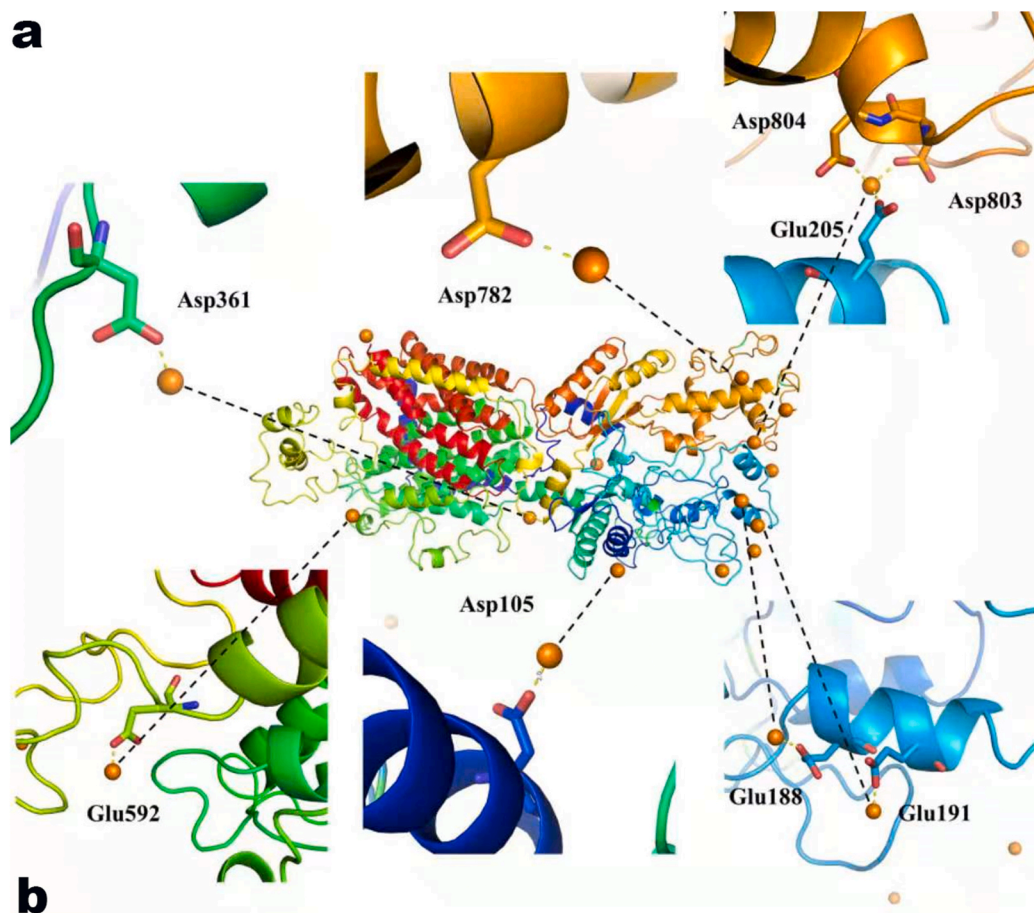
**Fig. 9.** a: Molecular dynamics simulation results. Mg2+ forms a coordination bond with Glu592, Asp803, Asp804, Glu191, Glu188, Glu205, Asp782, Asp361, Asp105, and Asp787. b: Schematic diagram showing diffusion of implant-derived Mg2+ enhances bone consolidation in distraction osteogenesis via regulating Ptch protein activating Hedgehog-alternative Wnt signaling.

signaling is comprised of the ligand and cell surface molecules, Ptch and Smo [27]. Smo protein translocates into the primary cilium and leads to the activation of transcription factor Gli, which then translocates to the nucleus [28]. Among them, Gli1 and Gli2 act similarly at the protein level, and both can promote Wnt5b [29,30]. We performed RT-PCR, Western blot and immunohistochemical analysis results verification on key genes in the Hedgehog signaling. The PCR results showed that Ptch1 and Gli1 were highly expressed in the HP Mg group. In consistency with these studies, our result showed that HP Mg promotes the expression level of Ptch1 and Gli1 in the consolidation period according to the

Western blot assay and immunochemical analysis increased in the HP Mg group (Figs. 7 and 8). Therefore, we proposed that magnesium promotes distraction osteogenesis calcification through the Hedgehog-alternative Wnt signaling.

We further explored why the Hedgehog pathway is activated, and found that Ptch is one of the potential targets by consulting the literature. Qi X et al. reported that the high-affinity protein-protein interface between PTCH1 and Hh protein is organized by the highly conserved calcium and zinc-binding sites of Hh protein [31]. The cryo-electron microscopy and crystallographic studies by Gong X et al. showed that

the mature Hedgehog protein contains three divalent metal ion structures. These three divalent metal ions help the Ptch conformation change, thereby activating Hedgehog signaling [32]. Hitzenberger M et al. through molecular dynamics experiments proved that Ca ions play an essential role in the stability of the Ptch loop regions where they are coordinated [33].Therefore, it can be assumed that magnesium ion, which is also a divalent metal ion, replaces the structure of Hp protein with Ptch through some mechanism, changes its protein conformation and function, reduces the inhibition of Smo, and further activates the Hedgehog pathway. Therefore, we evaluated the effect of Mg2+ ion on the structure of human ptch1 protein through molecular dynamics simulation. The results showed that Mg2+ forms a coordination bond with acidic amino acid residues Glu592, Asp803 and Asp804 on the surface of Ptch1 protein, which stabilizes the structure of the regions 562–595 and 794–803. It also forms coordination bonds with other acidic residues Glu191, Glu188, Glu205, Asp782, Asp361, Asp105, and Asp787, which also plays an important role in stabilizing the structure of Ptch1 protein (Fig. 9a). Therefore, we proposed that magnesium promotes distraction osteogenesis consolidation via regulating Ptch protein activating Hedgehog-alternative Wnt signaling.

Although in our work the biodegradable HP Mg pins have been proved as the potential application for DO, there are still some challenges for the clinical application. First, the problem of disintegration of mechanical integrity and local hydrogen accumulation should be solved [34,35]. Second, more biosafety tests should be performed to identify the products suitable for the use of the DO.

## 5. Conclusion

In this study, Hp Mg pin was applied in distraction osteogenesis model for enhance bone consolidation. Mechanical test, radiological and histological analysis suggested that Hp Mg pin can promote distraction osteogenesis and shorten the consolidation time. Further RNA sequencing investigation found that alternative Wnt signaling was activated. In further bioinformatics analysis, it was found that the Hedgehog pathway is the upstream signaling pathway of the alternative Wnt pathway. We found that Ptch protein is a potential target of magnesium and verified by molecular dynamics that magnesium ions can bind to Ptch protein. In conclusion, Hp Mg implants have the potential to enhance bone consolidation in the DO application, and this process might be via regulating Ptch protein activating Hedgehog-alternative Wnt signaling (Fig. 9b).

## Declaration of competing interest

We declare that we have no financial and personal relationships with other people or organizations that can inappropriately influence our work, there is no professional or other personal interest of any nature or kind in any product, service and/or company that could be construed as influencing the position presented in, or the review of, the manuscript entitled.

## CRediT authorship contribution statement

**Musha Hamushan:** Conceptualization, Methodology, Writing - original draft, Writing - review & editing. **Weijie Cai:** Methodology, Writing - review & editing. **Yubo Zhang:** Methodology, Writing - review & editing. **Zun Ren:** Methodology, Data curation. **Jiafei Du:** Methodology. **Shaoxiang Zhang:** Methodology, Supervision. **Changli Zhao:** Funding acquisition, Writing - review & editing. **Pengfei Cheng:** Data curation, Funding acquisition. **Xiaonong Zhang:** Conceptualization, Supervision. **Hao Shen:** Conceptualization, Supervision. **Pei Han:** Conceptualization, Funding acquisition, Supervision.

## References

[1] A. Nauth, E. Schemitsch, B. Norris, Z. Nollin, J.T. Watson, Critical-size bone defects: is there a consensus for diagnosis and treatment? J. Orthop. Trauma 32 (2018) S7.

[2] J.G. Birch, A brief history of limb lengthening, J. Pediatr. Orthop. 37 (Suppl 2) (2017) S1–S8.

[3] M. Singh, A. Vashistha, M. Chaudhary, G. Kaur, Biological Basis of Distraction Osteogenesis – A Review 28 (2016) (2016) 1–7.

[4] C.M. Runyan, K.S. Gabrick, Biology of bone formation, fracture healing, and distraction osteogenesis, J. Craniofac. Surg. 28 (2017) 1380–1389.

[6] S.J. Kempton, J.E. Mccarthy, A.M. Afifi, A systematic review of distraction osteogenesis in hand surgery: what are the benefits, complication rates, and duration of treatment? Plast. Reconstr. Surg. 133 (2014) 1120–1130.

[7] U. Spiegl, R. Pätzold, J. Friederichs, S. Hungerer, M. Militz, V. Bühren, Clinical course, complication rate and outcome of segmental resection and distraction osteogenesis after chronic tibial osteitis, Injury 44 (2013) 1049–1056.

[8] S. Sabharwal, S.C. Nelson, J.K. Sontich, What's new in limb lengthening and deformity correction, J. Bone Joint Surg. Am. 97 (2015) 1375–1384.

[9] P. Hong, D. Boyd, S.D. Beyea, M. Bezuhly, Enhancement of bone consolidation in mandibular distraction osteogenesis: a contemporary review of experimental studies involving adjuvant therapies, J. Plast. Reconstr. Aesthetic Surg. 66 (2013) 883–895.

[10] Biodegradable magnesium-based implants in orthopedics—a general review and perspectives, Advanced ence 7 (2020).

[11] J. Zhang, L. Tang, H. Qi, Q. Zhao, Y. Liu, Y. Zhang, Dual function of magnesium in bone biomineralization, Adv Healthc Mater (2019), e1901030.

[12] Y. Yu, H. Lu, J. Sun, Long-term in vivo evolution of high-purity Mg screw degradation - local and systemic effects of Mg degradation products, Acta Biomater. 71 (2018) 215–224.

[13] P. Cheng, P. Han, C. Zhao, S. Zhang, H. Wu, J. Ni, et al., High-purity magnesium interference screws promote fibrocartilaginous entheses regeneration in the anterior cruciate ligament reconstruction rabbit model via accumulation of BMP-2 and VEGF, Biomaterials 81 (2016) 14–26.

[14] P. Han, P. Cheng, S. Zhang, C. Zhao, J. Ni, Y. Zhang, et al., In vitro and in vivo studies on the degradation of high-purity Mg (99.99wt.%) screw with femoral intracondylar fractured rabbit model, Biomaterials 64 (2015) 57–69.

[15] M. Hamushan, W. Cai, Y. Zhang, T. Lou, S. Zhang, X. Zhang, et al., High-purity magnesium pin enhances bone consolidation in distraction osteogenesis model through activation of the VHL/HIF-1α/VEGF signaling 35 (2020) 224–236.

[16] Xu Yiran, Sun Yanyan, Zhou Kai, et al., Cranial irradiation induces hypothalamic injury and late-onset metabolic disturbances in juvenile female rats, Dev. Neurosci. 40 (2018) 120–133.

[17] Y. Komiya, R. Habas, Wnt signal transduction pathways, Organogenesis 4 (2008) 68–75.

[18] WNT signaling in bone homeostasis and disease: from human mutations to treatments, Nat. Med. 19 (2013) 179–192.

[19] Y. Kobayashi, K. Maeda, N. Takahashi, Roles of Wnt signaling in bone formation and resorption, Jpn Dent Sci Rev 44 (2008) 76–82.

[20] C.C. Hung, A. Chaya, K. Liu, K. Verdelis, C. Sfeir, The role of magnesium ions in bone regeneration involves the canonical Wnt signaling pathway, Acta Biomater. 98 (2019) 246–255.

[21] H.W. Park, Y.C. Kim, B. Yu, T. Moroishi, J.S. Mo, S.W. Plouffe, et al., Alternative wnt signaling activates YAP/TAZ, Cell 162 (2015) 780–794.

[22] I.T. Ling, L. Rochard, E.C. Liao, Distinct requirements of wls, wnt9a, wnt5b and gpc4 in regulating chondrocyte maturation and timing of endochondral ossification, Dev. Biol. 421 (2017) 219–232.

[23] B.A. Alman, The role of hedgehog signalling in skeletal health and disease, Nat. Rev. Rheumatol. 11 (2015) 552–560.

[24] S. Onodera, A. Saito, H. Hojo, T. Nakamura, D. Zujur, K. Watanabe, et al., Hedgehog activation regulates human osteoblastogenesis, Stem Cell Rep. 15 (2020) 125–139.

[25] J. Yang, P. Andre, L. Ye, Y.Z. Yang, The Hedgehog signalling pathway in bone formation, Int. J. Oral Sci. 7 (2015) 73–79.

[26] X. Liu, J.A. McKenzie, C.W. Maschhoff, M.J. Gardner, M.J. Silva, Exogenous hedgehog antagonist delays but does not prevent fracture healing in young mice, Bone 103 (2017) 241–251.

[27] K. Petrov, B.M. Wierbowski, A. Salic, Sending and receiving hedgehog signals, Annu. Rev. Cell Dev. Biol. 33 (2017) 145–168.

[28] M. Xin, X. Ji, L.K. De La Cruz, S. Thareja, B. Wang, Strategies to target the Hedgehog signaling pathway for cancer therapy, Med. Res. Rev. 38 (2018) 870–913.

[29] Y. Zhang, D.P. Bulkley, Y. Xin, K.J. Roberts, D.E. Asarnow, A. Sharma, et al., Structural basis for cholesterol transport-like activity of the hedgehog receptor patched, Cell 175 (2018) 1352–1364, e14.

[30] C. Zhang, Y. Yuan, L. Fang, Y. Xuan, Promotion of osteogenesis by bioactive glass-ceramic coating: possible involvement of the Hedgehog signaling pathway, J. Orthop. Sci. 24 (2019) 731–736.

[31] X. Qi, P. Schmiege, E. Coutavas, X. Li, Two Patched molecules engage distinct sites on Hedgehog yielding a signaling-competent complex, Science (2018) 362.

[32] X. Gong, H. Qian, Structural Basis for the Recognition of Sonic Hedgehog by Human Patched1, 2018, p. 361.

[33] M. Hitzenberger, T.S. Hofer, The influence of metal-ion binding on the structure and surface composition of Sonic Hedgehog: a combined classical and hybrid QM/MM MD study, Phys. Chem. Chem. Phys. 18 (2016) 22254–22265.

[34] N. Sezer, Z. Evis, S.M. Kayhan, A. Tahmasebifar, M. Koç, Review of magnesium-based biomaterials and their applications, J. Magn. Alloys 6 (2018) 23–43.

[35] J. Walker, S. Shadanbaz, T.B.F. Woodfield, M.P. Staiger, G.J. Dias, Magnesium biomaterials for orthopedic application: a review from a biological perspective, J. Biomed. Mater. Res. B Appl. Biomater. 102 (2014) 1316–1331.